ESA SEPEM Project: Peak Flux and Fluence Model

Piers T. A. Jiggens, Stephen B. Gabriel, *Member, IEEE*, Daniel Heynderickx, Norma Crosby, Alexi Glover, and Alain Hilgers

***Abstract*—A new modeling methodology for the prediction of the solar proton environment a 1 AU developed as part of the Solar Energetic Particle Environment (SEPEM) Project for the European Space Agency (ESA) is presented. This new method named *Virtual Timelines* is applied to the SEPEM Reference Event List derived from a long flux time series of space-based measurements to produce the SEPEM model for proton peak flux and fluence at 1 AU. There are several new components including the use of the Lévy distribution for time distributions and the accounting for the non-point-like nature of SEP events.**

***Index Terms*—Fluence, peak flux, probabilistic model, solar energetic particles (SEPs), statistical model.**

I. Introduction

SOLAR energetic particles (SEPs) are accelerated in the solar corona (and interplanetary space) releasing energy previously stored in the strong magnetic fields. Solar flares may be responsible for small increases in SEPs, but the major increases in solar protons result primarily from coronal mass ejections (CMEs), although these are often accompanied by associated flaring. A review of the different particle acceleration mechanisms and resulting particle compositions from CME-driven shocks and solar flares is given by Reames [1].

In this paper, we focus on solar protons that are known to cause displacement damage, single-event upsets (SEUs), and total dose effects. Heavy ions can cause similar effects; modeling heavy ions can be done either by using the same method as for the protons [2] or by an extrapolation method based on the results for solar protons [3]. A review of the causes of space weather and their effects is given by Feynman and Gabriel [4].

To enable spacecraft designers to mitigate for the effects of SEPs, statistical, probabilistic models providing predictions of the cumulative fluences and the highest fluences or peak fluxes resulting from a single event to be seen over a user-specified mission duration as a function of confidence level have been constructed. These environment models are based on previous observations and combine fits of distributions to the event fluxes (both peak intensities and integrated) and to the time distribution of SEP events.

The first widely accepted model for solar proton fluences was that of King [5]. King divided events of cycle 20 into anomalously large (AL), of which there was only one (August 1972), and ordinary (OR) events and used Burrell extended Poisson statistics to model their occurrence separately. The AL events dominated the results, so it is often reasoned that the King model is based on this single historical event. However, the OR events were modeled using a normal distribution fit to $\log_{10}$ of the fluences, and this was combined with the Poisson-based time distribution to generate this component of the model. This methodology is similar to that applied in all variants of the JPL solar proton models [6]–[9], which are probably the most widely used by spacecraft designers to date. All these models predict mission cumulative fluences for a given confidence over a range of energies at the Earth (1 AU). Confidence is the certainty with which it can be said a fluence value will not be exceeded. A large number of Monte Carlo runs are performed combining distributions of SEP event frequency and SEP event fluence. The generated event fluences are then summed to generate the cumulative fluence for each iteration. The iterations are then sorted and plotted against a vector with uniformly spaced elements of the same length with range [0, 1] which represents the likelihood that the corresponding fluence will be exceeded. If a user wished to calculate the fluence for the 90% confidence level (10% likelihood of being exceeded), this would be the value that 90% of the Monte Carlo runs' fluences were lower and only 10% were greater. These fluences vary depending on the mission length with a longer mission length having a different event frequency probability density function (pdf) to reflect this.

The MSU model [10] follows a similar method to that of King with three key differences. The first of these is that a power-law distribution is applied to model the fluences rather than a log-normal distribution. The second difference is that the event fluence energy spectra is determined using a probability model of spectral shape extrapolated from the >30 MeV fluence distribution that is modeled directly in the MSU model, whereas the King and JPL models use different event frequency and fluence distributions for different energy ranges. The data for higher energies are limited as fewer events have been seen. However, there is also high variability of spectra between different SEP events [11], so both techniques have drawbacks. The last difference is that the MSU Model determines the event frequency with a solar cycle dependence based on sunspot (Wolf) number rather than assuming that event frequency can be treated as invariant over seven solar active years per cycle and that the fluence from SEP events during the four remaining quiet years are not significant by comparison. The correlation between sunspot

Manuscript received October 27, 2011; revised February 03, 2012 and March 30, 2012; accepted April 21, 2012. Date of publication June 06, 2012; date of current version August 14, 2012. This work was supported by the European Space Agency Technology Research Programme under ESA Contract No. 20162/06/NL/JD.

P. T. A. Jiggens and A. Hilgers are with the ESA/ESTEC, Noordwijk 2200 AG, The Netherlands (e-mail: piers.jiggens@esa.int).

S. B. Gabriel is with the University of Southampton, Southampton SO17 1BJ, U.K.

D. Heynderickx is with the DH Consultancy, Leuven 3000, Belgium.

N. Crosby is with the BIRA, Brussels 1180, Belgium.

A. Glover is with the ESA/ESAC, Madrid 28692, Spain.

Color versions of one or more of the figures in this paper are available online at http://ieeexplore.ieee.org.

Digital Object Identifier 10.1109/TNS.2012.2198242

number and event frequency has been strongly contested (see [8] and [10]).

A distinctly separate methodology for modeling the SEP environment is the ESP method [12], which, assuming a Poisson distribution of events, uses an analytical extension based on the distribution of one-year fluences (found to be lognormal using the Maximum Entropy Principle) to estimate multiyear cumulative fluence probability distribution. This reduces the heavy dependence on a few SEP events and also mitigates the need to consider the duration of events to create a realistic modeling scenario. However, the number of data points that can be used is limited to the number of years for which there are data rather than the far higher number of SEP events that have been observed; this limits the reliability of the model results. Xapsos *et al.* [13], [14] also provided an analytical way of combining distribution functions for worst-case peak flux and event fluence, determined using Maximum Entropy Theory to be described by truncated power laws, with a Poisson (random) event occurrence assumption avoiding the necessity of performing a large number of iterations. This can only be used for the worst-case SEP event fluences [14] and peak fluxes [15] rather than the cumulative fluence model.

All of the above methods use the Poisson distribution to model the occurrence of SEP events, although the way in which this is done varies. It has been shown that the Lévy distribution is a more appropriate, robust distribution for modeling SEP occurrence [16]. The modeling method described in this paper makes use of this prior work. Separate waiting time distributions are used for solar maximum and solar minimum. Recent large events such as that in December 2006 [17] occurred at solar minimum highlighting the need for models to account for these periods.

Feynman *et al.* [18] used time blocks of 60 days combined with assumptions of radial dependence of fluences to estimate the fluence that might be seen by the Solar Probe mission, which is intended to travel to three solar radii of the solar surface and is to be launched in approximately 2015. No distribution was fit to the time blocks in this case, making it an example of a purely data-driven model that does not require event definition or an assumed distribution for event frequency. This is a benefit for short mission durations, but due to limited data is not appropriate for longer missions. Jun *et al.* [19] extended this method by generating and extended timeline of pseudo-events based on the same distributions as used for the JPL model.

Kim *et al.* [20] modeled the occurrence of large SEP events on a Poisson process that was nonhomogeneous, i.e., for which the mean event rate varied over the solar cycle. This was combined with an empirical distribution function to predict the distribution of doses to be seen in typical blood-forming organs of astronauts.

In this paper, a new model for solar protons developed for the Solar Energetic Particle Environment Modelling (SEPEM) Project for the European Space Agency (ESA) is presented. The methodology is introduced in Section II, the data used are detailed in Section III, the selection of time and flux distributions are explained in Sections IV and V, respectively, regression of event duration with flux is performed in Section VI, followed by results (Section VII), discussion (Section VIII), and conclusion (Section IX).

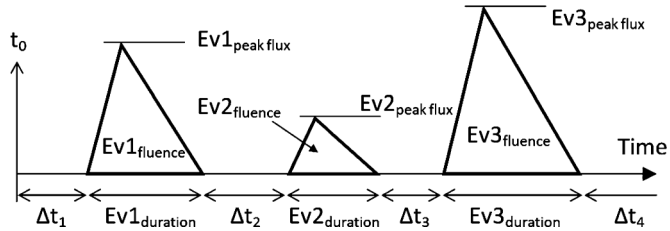

Fig. 1. Cartoon representing the Virtual Timeline method where Δ_n is the waiting time prior to event Evn, which has corresponding peak flux or fluence as shown.

II. Methodology

In this paper a new, alternative method for modeling the SEP environment called *Virtual Timelines* is presented. Here, the distribution of waiting times (defined as the time from the end of one event to the onset of the following event) is used as opposed to the event frequency. These distributions are complementary, and a Fourier transform of the event frequency will result in the event waiting time. However, by using the event waiting times, it is possible to incorporate the duration of events that are not point-like in their nature. The assumption that events are point-like is made implicitly in all previous models with the exception of recent work by Jun *et al.* [19]. The data-driven model of Feynman *et al.* [18] and the cumulative fluence model of Xapsos *et al.* [12] do not require to consider event durations as they do not generate events as part of their methodologies.

The inclusion of event waiting times allows for more realistic scenarios in model iterations accounting for the dependency of event durations on the fluence (peak flux). Furthermore, using virtual timelines allows the modeler to alter the nature of the environment during a model run (or iteration). For example, this would allow the effective combination of periods of high solar activity (solar maximum) with quieter periods (solar minimum). Fig. 1 shows a cartoon of the *Virtual Timeline* methodology.

Each timeline comprises waiting times (times between events) and events interspersed. The waiting times are randomly generated using a distribution fitted to the sample event list waiting times. Event fluence or peak flux values are randomly generated from a fitted distribution, and then a semi-empirical regression technique with random scatter is used to generate a duration for the event based on this value.

It is implicitly assumed that, over solar maximum, there is no correlation between waiting time and event fluence, which simplifies the model. Were the waiting time defined from the onset of one event to the onset of the following event, larger events would have a longer minimum waiting time proceeding them, which would need to be accounted for.

III. Data

For protons, the energy range of interest was established at a round-table meeting of experts and users, held at the University of Southampton, Southampton, U.K., in February 2007 as being from 5 to 200 MeV. To reduce uncertainty, model parameters should be derived from as long a time period as possible

for which the proton flux time series are available. Proton flux data from two well-known spacecraft [The Interplanetary Monitoring Platform -8 (IMP-8) and spacecraft Geostationary Operational Environmental Satellite (GOES)] have been used for this study.

The IMP-8/GME (Goddard Medium Energy) instrument was selected as it has a long time of operation (1973–2001) and good energy discrimination, however it suffers from saturation, data gaps, and poor time resolution (30 min). The GOES/SEM(-2) (Space Environment Monitor) has poorly resolved energy bins, but importantly does not saturate, has very few data gaps, and usually there have been two GOES spacecraft in operation at any given time.

As saturation is a very important issue for an engineering model of the SEP environment, the GOES/SEM data were used from 1986–2009. Earlier work by Rosenqvist *et al.* [9] showed that the most reliable datasets for deriving SEP event fluence were those from GOES-7 and GOES-8, therefore they were used preferentially. From 1973–1985, as the observed SEP events did not have high fluxes saturation in the GME instrument was not an issue, so these data were used for this period. Rosenqvist *et al.* [9] demonstrated cross calibration of solar proton data to create a more homogeneous time series. This idea was developed to calibrate the GOES/SEM data with the IMP-8/GME data using points where the data overlapped and was of good quality in both cases. To enable this, it was necessary first to rebin the data into standard energy bins. To avoid bias, it was decided to create 10 new bins exponentially distributed covering the range from 5 to 200 MeV—the "SEPEM Standard Energy Channels." This rebinning was done point-by-point using a piecewise power law to interpolate between the two closest energies in the raw data of both SEM and GME. This calibration of the GOES/SEM data with the IMP-8/GME data established of the proper spectral separation for GOES/SEM data, corrected for known response errors in GOES/SEM data (see [9]), and reduced the background level. Calibration of the nonsaturating GOES/SEM data with the scientific IMP-8/GME instrument data (where it was not saturated) corrects for response errors while providing a continuous time series without saturation taking advantage of the best features of each instruments' data. Due to the reduction in the background resulting from the cross calibration, further background flux subtraction was not deemed necessary as the remaining background was negligible during SEP events and periods between events are not included in the modeling. Table I shows the data used for the various time periods to produce a reliable and contiguous time series of proton flux.

TABLE I
TABLE OF PRIMARY DATASETS USED

Instrument	Start Date	End Date
IMP-8/GME	11/1973	12/1985
GOES-5/SEM	01/1986	02/1987
GOES-7/SEM	03/1987	02/1995
GOES-8/SEM	03/1995	05/2003
GOES-11/SEM	06/2003	06/2009

A. Event Definition

With a continuous, homogenous, flux time series covering 35.66 years established, the next step was to extract the periods of interest, i.e., the SEP events. Events were defined as beginning when the flux in the second SEPEM energy channel (7.23–10.46 MeV) went above 0.01 $\mathrm{cm^{-2}s^{-1}sr^{-1}MeV^{-1}}$. Use of this channel ensured that all periods where there were significant flux increases resulting from solar origin in any channel were detected, while the energy range was also high enough to be certain that none of the increases resulted from trapped radiation or electron contamination. Use of this very low flux threshold was possible due to the quality of the cleaned data and minimized the chance of missing higher-energy particles, a significant portion of which can arrive earlier than the 7.23–10.46 MeV proton flux reaches higher levels.

As reported by Feynman *et al.* [6] and Tylka *et al.* [2], consecutive flux enhancements may not be independent in time, and treating them as separate events results in the model systematically underpredicting the likelihood of such sequences. To mitigate this, a minimum dwell time of 24 h was introduced such that if the flux rose above 0.01 $\mathrm{cm^{-2}s^{-1}sr^{-1}MeV^{-1}}$ again within 24 h of the end of an event, the enhancements were treated as the same event. As a result events are generally longer in time with a lower average frequency than those in the National Oceanographic and Atmospheric Administration (NOAA) SEP event list.[1]

Due to some remaining noise on the background produced either by noneruptive phenomena or from within the instrument, many small enhancements not of solar origin were detected. A minimum event duration of 24 h and a minimum peak flux (intensity) of 0.5 $\mathrm{cm^{-2}s^{-1}sr^{-1}MeV^{-1}}$ were introduced to remove erroneous and insignificant events.

A parametric study was carried out to test the robustness of the event definition selected to ensure that small changes in the definition did not result in large changes in the model results. This energy channel the events were defined in was altered, and the dwell time, minimum event duration, and flux thresholds were varied. Very small changes in parameters had no effect on the event list and therefore the model results. A moderate reduction in, for example, the dwell time increased the number of events, but this was largely offset by the impact on the event flux distribution in the final model results. However, large changes in parameters could affect model results due to a failure to include all significant periods, inclusion of high percentage of quiet periods within events, or a resulting disregard for interevent dependencies made significant by the changes. The results for various SEP environment models were investigated.

The final SEPEM Reference Event List includes 225 events at an average of 6.3095 per year, of which 194 are in active years (9.2381 per year) and 31 are at solar minimum (2.1145 per year).[2]

B. Peak Flux and Fluence Thresholds

The event list includes all events that could be significant in terms of their peak flux or their integrated flux (fluence) values in any of the 10 energy channels. Only a fraction of these would be significant for either parameter at any one energy, and in

[1]http://umbra.nascom.nasa.gov/SEP/

[2]http://dev.sepem.oma.be/help/event_ref.html

TABLE II
TABLE OF ENERGY CHANNELS AND THRESHOLDS

Ch.	Energy (MeV)	Peak Flux	Fluence
1	5.00 - 7.23	1.0000E+1	3.1623E+5
2	7.23 - 10.46	3.1623E+0	1.0000E+5
3	10.46 - 15.12	1.0000E+0	3.1623E+4
4	15.12 - 21.87	3.1623E-1	1.0000E+4
5	21.87 - 31.62	1.0000E-1	3.1623E+3
6	31.62 - 45.73	3.1623E-2	1.0000E+3
7	45.73 - 66.13	1.0000E-2	3.1623E+2
8	66.13 - 95.64	3.1623E-3	1.0000E+2
9	95.64 - 138.3	1.0000E-3	3.1623E+1
10	138.3 - 200.0	3.1623E-4	1.0000E+1

order to create these subgroups of events, flux thresholds were required. Rather than risk biasing the results by handpicking these thresholds, it was decided that there should be an analytical spectra established for the flux and fluence thresholds. After investigation, it was found that the most appropriate formula was a power law given by

$$TH_{\mathrm{PkF(Flu)}} = A_{\mathrm{PkF(Flu)}} E^{-b} \tag{1}$$

where TH is the peak flux (PkF) or fluence (Flu) threshold at a given energy, E, b is the (negative) gradient of the power law, and A is a constant related to the intercept of a straight line fit to the logarithms of the thresholds. This allows automatic determination of thresholds for energy ranges that are intermediate between the energy channels used to bin the data in SEPEM.

The exponent b is defined as the gradient after taking logarithms using as input only appropriate threshold values for the first and last channels for either fluence or peak flux

$$b = \frac{\ln(10^{5.5}) - \ln(10)}{\ln\sqrt{200 \times 138.3} - \ln\sqrt{7.23 \times 5}} = \frac{\ln(10) - \ln(10^{-3.5})}{\ln\sqrt{200 \times 138.3} - \ln\sqrt{7.23 \times 5}} = 3.1209.$$

The geometric mean is used to define a channel's energy. The constant A_{PkF} is the intercept value after taking natural logarithms applying b to the peak flux threshold of any energy (here the mean of the first channel is used)

$$A_{\mathrm{PkF}} = \exp(\ln(10) + (b \ln\sqrt{7.23 \times 5})) = 2.70 \times 10^3.$$

Likewise, the constant A_{Flu} is the intercept value after taking natural logarithms applying b to the fluence threshold of any energy (here, the mean of the first channel is used)

$$A_{\mathrm{Flu}} = \exp(\ln(10^{5.5}) + (b \ln\sqrt{7.23 \times 5})) = 8.54 \times 10^7.$$

Table II shows the 10 energy channels used in SEPEM to bin the data along with the peak flux and fluence thresholds used to define the significant events in each channel for this work. These thresholds are distinct from the thresholds used to define the events explained in Section III-A.

IV. FITS TO TIME DISTRIBUTIONS

The event waiting times (defined as the time from the end of one event to the start of the next) and event durations were fit with a Poisson distribution, a time-dependent Poisson distribution, and a Lévy distribution. The bins were selected to be exponentially distributed, with the lowest bin limit equal to the shortest time in the event list and the highest 20% higher than the longest time and the number of bins equal to the number of events divided by 25 (rounded up). In this way, there was no biasing of the data to favor one distribution or another.

TABLE III
WAITING TIME DISTRIBUTION PARAMETERS

	Lévy Parameters		Poisson	Time-Dependent Poisson
	μ	c	λ	ϱ
Solar Max.	0.2629	14.543	0.0205	0.0257
Solar Min.	-	-	0.0058	0.0058

The expression of a Poisson process in the time domain, or waiting time (duration) distribution, is equal to the pdf of the exponential distribution

$$P(\Delta t) = \lambda e^{-\lambda \Delta t} \tag{2}$$

where $P(\Delta t)$ is the probability density for a waiting time (duration) Δt for an average event frequency λ.

Wheatland applied the time-dependent Poisson distribution to solar-flare waiting times [21] and CME waiting times [22] given by

$$P(\Delta t) = \frac{2\varrho}{(1 + \varrho \Delta t)^3} \tag{3}$$

where $P(\Delta t)$ is the probability density for a waiting time (duration) Δt for an average event frequency ϱ.

The Lévy distribution probability density fit to SEP event waiting times [16] is given by

$$P(\Delta t) = \exp(-|c\Delta t|^{\mu}) \tag{4}$$

where $P(\Delta t)$ is the probability density for a waiting time (duration) Δt, μ is the characteristic exponent, and c is the scaling factor. Integration of the above function allows random sampling of the Lévy distribution; this must be done numerically.

A. Waiting Times

Table III shows the distribution parameters for the functions fit to the waiting times. Fig. 2 shows the Poisson distribution, time-dependent Poisson distribution, and Lévy distribution fits to the waiting times. It shows close agreement between the fits for the time-dependent Poisson distribution and for the Lévy distribution.

Table IV shows the goodness-of-fit parameters for the waiting time distributions for the SEPEM Event List. S^2 is the sum of squared residuals applied to the natural logarithms of the binned values, and χ^2 is the chi-squared parameter for the residuals. The fits were determined by minimizing a combination of these two goodness-of-fit parameters; the reason for this choice and more explanation about the parameters is given in [16]. This shows that the Lévy distribution and time-dependent Poisson distributions are the best fitted to the data. In previous work [16] using three event lists generated using different event definitions, it was found that the Lévy distribution was found to be

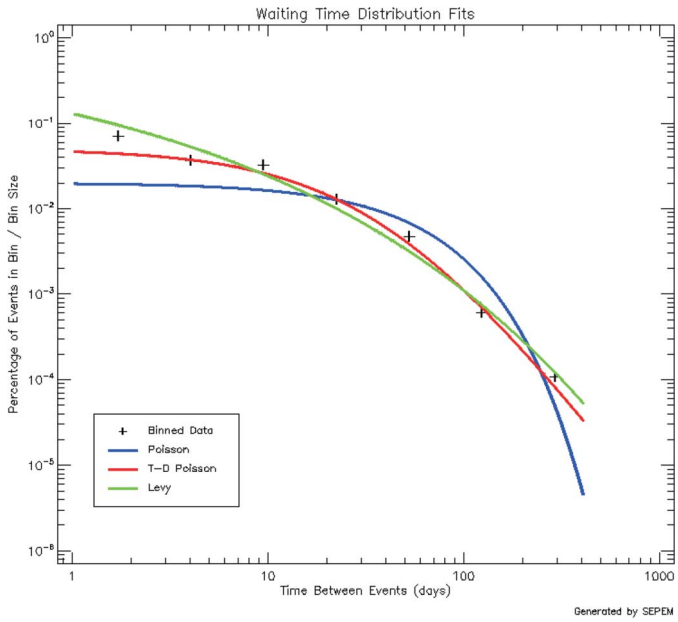

Fig. 2. Fittings to waiting times for SEPEM Reference Event List.

TABLE IV
WAITING TIME DISTRIBUTION GOODNESS-OF-FIT

	Lévy	Poisson	Time-Dependent Poisson
S^2	0.5531	4.1859	0.3920
χ^2	0.0154	0.1707	0.0175

the most robust distribution to be used for both the waiting times and the durations. The time-dependent Poisson distribution produces a similar result with one fewer free parameter, and in statistics parsimony (the minimization of free parameters) is desirable. However, there is a tendency for the time-dependent Poisson distribution to underpredict the likelihood of short waiting times and overpredict the likelihood of long waiting times, which might result in underprediction of the severity of the environment, which is dangerous when considering the design of expensive spacecraft. For these reasons, the Lévy distribution is applied in the SEPEM model to the waiting times for the active year periods.

Unfortunately, due to the sparsity of events during the quiet years (or solar minimum), it is not possible to perform a good fit to the binned waiting times, meaning the same method applied to the waiting times during active years cannot be applied to quiet years. However, the mean rate of SEP events (per day) in the event list can be used as the parameter ρ in the time-dependent Poisson distribution (3) or λ in the Poisson distribution. This value is shown in Table III. At these times when events are rarer, the drawbacks of underpredicting very high event rates using this distribution are not so keenly felt, and therefore it was decided to use the time-dependent Poisson distribution in the SEPEM model for solar quiet years (solar minimum).

B. Event Durations

The event durations fits were performed in the same way as for waiting times, but separately for each of the peak flux and fluence distributions in each of the 10 energy channels. These fits include only those events exceeding the thresholds shown in Table II. Table V shows the goodness-of-fit parameters for the duration distributions for events above the fluence and peak flux thresholds for each channel. In 13/20 of the cases, the Lévy distribution fit was the best of the three tested, and the sum of the goodness-of-fit parameters over the 10 channels was lower applying both fluence and peak flux thresholds. Event durations were limited to a maximum of the largest seen in the sample data (45 days) using the event definition elaborated in Section III-A. Allowing for very long event durations could result in an underprediction of mission fluxes by consuming a disproportionately large section of the timeline generated. It was decided to be conservative rather than risk underprediction.

The goodness-of-fit parameter is the square root of the χ^2 multiplied by the sum of the squared residuals after taking natural logarithms. This is the same as used in previous work [16], and the reasons for the choice of this combined parameter are given in that paper.

One reason that the Lévy distribution generally provides better fits is that it permits a limited range of event durations, and the event list has a minimum duration of 24 h. It is necessary that the area under the curve sums to 1 (100% of all possible outcomes). By setting the maximum duration equal to the maximum seen in the event list, this requirement determines the minimum duration, which, as can be seen from Fig. 3, is very close to 24 h, thus indicating that the derived cumulative distribution function is appropriate.

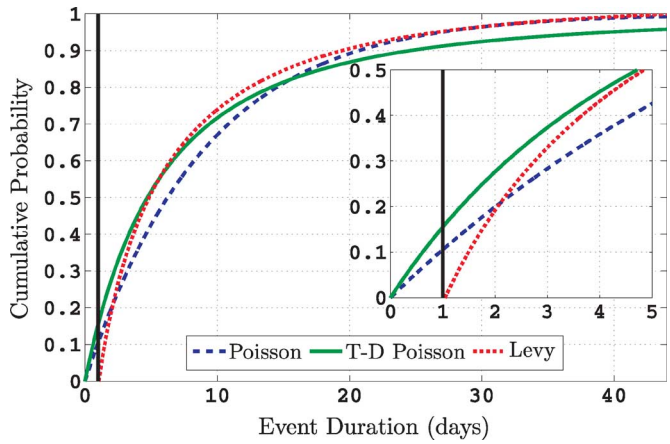

Fig. 3. Cumulative distribution functions for durations for channel-5 events.

TABLE V
DURATION DISTRIBUTION GOODNESS-OF-FIT FOR EVENTS ABOVE THE FLUENCE AND PEAK FLUX THRESHOLDS

	Peak Flux			Fluence		
	Lévy	Poisson	T-d Pois	Lévy	Poisson	T-d Pois
1	0.0097	0.0177	0.0142	0.0125	0.0334	0.0258
2	0.0059	0.0242	0.0101	0.0170	0.0452	0.0331
3	0.0016	0.0507	0.0128	0.0290	0.0335	0.0358
4	0.0017	0.0466	0.0133	0.0027	0.0326	0.0116
5	0.0081	0.0083	0.0067	0.0198	0.0074	0.0116
6	0.0026	0.0212	0.0091	0.0108	0.0123	0.0106
7	0.0067	0.0065	0.0056	0.0167	0.0034	0.0073
8	0.0027	0.0140	0.0073	0.0075	0.0046	0.0053
9	0.0013	0.0470	0.0182	0.0068	0.0048	0.0047
10	0.0016	0.0211	0.0093	0.0054	0.0074	0.0055
Sum	0.0419	0.2573	0.1067	0.1281	0.1847	0.1514

TABLE VI
LOGNORMAL DISTRIBUTION FITTED PARAMETERS

	Peak Flux		Fluence	
Ch.	μ	σ	μ	σ
1	4.50E+0	2.37E+0	1.52E+1	2.10E+0
2	3.37E+0	2.55E+0	1.40E+1	2.40E+0
3	2.35E+0	2.65E+0	1.30E+1	2.63E+0
4	1.38E+0	2.79E+0	1.19E+1	2.88E+0
5	3.70E-1	2.62E+0	1.07E+1	2.86E+0
6	-1.00E+0	2.88E+0	9.27E+0	3.18E+0
7	-2.08E+0	2.97E+0	8.34E+0	3.25E+0
8	-3.16E+0	2.85E+0	7.28E+0	3.06E+0
9	-4.65E+0	2.86E+0	5.27E+0	3.20E+0
10	-6.15E+0	3.09E+0	4.05E+0	3.20E+0

TABLE VII
TRUNCATED POWER LAW FITTED PARAMETERS

	Peak Flux		Fluence	
Ch.	b	$\phi_{\max}$	b	$\phi_{\max}$
1	2.98E+1	2.09E+4	2.62E+1	5.89E+8
2	2.90E+1	9.58E+3	2.56E+1	3.07E+8
3	2.72E+1	4.13E+3	2.39E+1	1.42E+8
4	2.55E+1	1.87E+3	2.29E+1	7.43E+7
5	2.39E+1	5.08E+2	2.30E+1	2.04E+7
6	2.56E+1	2.36E+2	2.62E+1	1.40E+7
7	2.52E+1	9.55E+1	2.36E+1	5.49E+6
8	2.30E+1	1.95E+1	2.38E+1	1.19E+6
9	2.64E+1	4.76E+0	3.15E+1	3.14E+5
10	2.90E+1	1.79E+0	3.32E+1	1.13E+5

V. FLUX DISTRIBUTIONS

For the peak flux and fluences for the SEP events, three distributions were investigated: the lognormal distribution, a truncated power law, and a power law with exponential cut-off.

A. Lognormal Distribution

The lognormal distribution was used (for the JPL model) by Feynman *et al.* [6]. This is actually the normal distribution applied to the $\log_{10}$ (rather than the natural logarithm) of the event fluences (peak fluxes) and is given by

$$F(\phi) = 1 - \frac{1}{2}\left(1 + \operatorname{erf}\left[\frac{\log_{10}(\phi) - \mu}{\sigma\sqrt{2}}\right]\right) \tag{5}$$

where $F(\phi)$ is the probability of a random event exceeding a fluence (peak flux) ϕ, and μ and σ are the mean and standard deviation of the $\log_{10}$ of the fluences (peak fluxes), respectively. ϕ and μ are not taken as the sample characteristics, but are fitted to the data.

There is a known departure at the lowest fluences that does not have a significant impact on model outputs. However, there is also a departure at higher fluence values using this distribution with the fit overpredicting the possibility of very high fluence (peak flux) events in all energy channels. This makes this choice of distribution conservative using the SEPEM Event List. Table VI shows the fitted parameters for the lognormal distribution.

B. Truncated Power Law

The second distribution investigated was the truncated power law used by Xapsos *et al.* [14], [15], which is given by

$$F(\phi) = 1 - \frac{\phi_{\min}^{-b} - \phi^{-b}}{\phi_{\min}^{-b} - \phi_{\max}^{-b}} = \frac{\phi^{-b} - \phi_{\max}^{-b}}{\phi_{\min}^{-b} - \phi_{\max}^{-b}} \tag{6}$$

where $F(\phi)$ is the probability of a random event exceeding a fluence (peak flux) ϕ, b is the power-law exponent, $\phi_{\min}$ is the fluence (peak flux) threshold given in Table II, and $\phi_{\max}$ is the maximum possible event fluence (peak flux) or "design limit." In the case of the truncated power law, b and $\phi_{\max}$ are the parameters determined by a best fit.

In general, this fit is very good. The one drawback is that the maximum event fluence is very close to the highest fluence value seen in the data. This indicates that over the 35.66-year time period, the largest possible event has been seen. It seems unlikely that this is the case especially when we consider historical events thought to exceed the largest event shown here such as the "Carrington Event" [23]. It should be pointed out that Xapsos *et al.* [14] found a maximum value for their >10 MeV data, which was comfortably in excess of the largest fluence in their event list, but for the carefully processed SEPEM data, this is not the case. Use of this distribution could lead to an underprediction of the severest scenario. Table VII shows the fitted parameters for the Truncated Power Law.

C. Cut-Off Power Law

The final distribution investigated was the cut-off power law used by Nymmik [24]

$$F(\phi) = \frac{\phi^{-\gamma}}{\exp\frac{\phi}{\phi_{\lim}}}\frac{\exp\frac{\phi_{\min}}{\phi_{\lim}}}{\phi_{\min}^{-\gamma}} \approx \frac{\phi^{-\gamma}\phi_{\min}^{\gamma}}{\exp\frac{\phi}{\phi_{\lim}}} (\phi_{\lim} \gg \phi_{\min}) \tag{7}$$

where $F(\phi)$ is the probability of a random event exceeding a fluence (peak flux) ϕ, γ is the power law exponent, $\phi_{\min}$ is the fluence (peak flux) threshold given in Table II, and $\phi_{\lim}$ is the exponential cut-off parameter that determines the deviation from a power law at high fluences (peak fluxes). In this case, the cut-off is gradual and determined by the exponential function of a fraction that only becomes significant at higher fluences, but unlike the truncated power law characteristic $\phi_{\max}$, this value can be exceeded, and the distribution therefore does not feature a "design limit." The intercept value C, used by Nymmik [24], is determined by the threshold given in Table II as opposed to being fitted.

These fits are very similar to that of the truncated power law used by Xapsos *et al.* [14]. However, in this case there is a smoother deviation from the pure power law allowing for the possibility of events significantly larger than those seen in the data. Table VIII shows the fitted parameters for the cut-off power law.

D. Fluence

To compare the fits illustrated above, a plot with logarithmic fluence but linear probability of a single event exceeding the stated fluence was used. The three fluence distribution fits for Channel 5 overlaid on the same axes are shown in Fig. 4. The inset of Fig. 4 displays the top end of the distribution with greater resolution; this shows the lognormal distribution

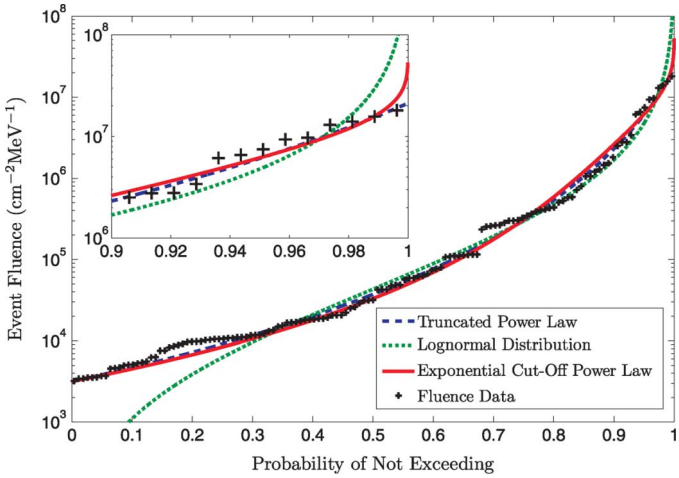

Fig. 4. Overlaid fittings to Channel-5 fluences.

TABLE VIII
CUT-OFF POWER LAW FITTED PARAMETERS

Ch.	Peak Flux		Fluence	
	γ	$\phi_{\lim}$	γ	$\phi_{\lim}$
1	3.47E+1	7.54E+3	3.14E+1	1.47E+8
2	3.42E+1	3.65E+3	3.14E+1	8.39E+7
3	3.30E+1	1.60E+3	3.01E+1	4.48E+7
4	3.23E+1	8.72E+2	2.90E+1	2.79E+7
5	3.14E+1	2.33E+2	2.95E+1	8.03E+6
6	3.23E+1	1.18E+2	3.04E+1	4.40E+6
7	3.14E+1	4.24E+1	2.84E+1	1.68E+6
8	3.04E+1	8.50E+0	2.92E+1	3.89E+5
9	3.24E+1	1.68E+0	3.55E+1	1.04E+5
10	3.35E+1	5.51E+1	3.63E+1	3.74E+4

TABLE IX
χ^2 GOODNESS-OF FIT PARAMETERS FOR EVENT FLUENCES

Ch.	Lognormal	Truncated P-L	Cut-Off P-L
1	6.001E+08	4.358E+08	9.418E+07
2	5.328E+08	1.392E+08	3.259E+07
3	4.002E+08	2.230E+07	1.693E+07
4	3.053E+08	1.387E+07	2.513E+07
5	7.349E+07	3.504E+06	6.227E+06
6	4.582E+07	2.687E+06	3.540E+06
7	1.893E+07	1.612E+06	1.678E+06
8	3.077E+06	1.443E+05	2.111E+05
9	5.666E+05	4.537E+04	2.968E+04
10	1.465E+05	1.095E+04	6.504E+03

systematically overpredicts the chances of very large events and, as stated previously, the maximum event size predicted by the truncated power law is very close to that of the sample. It therefore makes sense to select the cut-off power law for use in the model that lies in between the other two.

Table IX shows the χ^2 goodness-of-fit parameters for the three fitted fluence distributions. In five of the cases, the truncated power law was found to have the best fit, while the cut-off power law had the best fit in the remaining five cases. In all instances, the lognormal is the worst fitting distribution.

E. Peak Flux

The same process was followed for the peak fluxes of the events that exceeded the thresholds established above. Table X shows the χ^2 parameters for the three fitted peak flux distributions for the top half of the events only. Here, the cut-off power law is the best fit in six of the 10 cases, while the truncated power law is the best fit in the remaining four. In all but the first channel, the lognormal is the worst fitting distribution.

TABLE X
χ^2 GOODNESS-OF FIT PARAMETERS FOR EVENT PEAK FLUXES

Ch.	Lognormal	Truncated P-L	Cut-Off P-L
1	4.926E+08	4.931E+08	1.094E+08
2	4.064E+08	1.739E+08	4.135E+07
3	3.531E+08	2.632E+07	1.852E+07
4	2.832E+08	1.717E+07	2.600E+07
5	6.348E+07	4.546E+06	6.657E+06
6	4.087E+07	2.151E+06	3.511E+06
7	1.907E+07	1.701E+06	1.693E+06
8	3.181E+06	1.577E+05	2.129E+05
9	5.045E+05	3.237E+04	2.538E+04
10	1.369E+05	9.429E+03	7.227E+03

VI. DURATION REGRESSION WITH FLUX

Another requirement for the methodology is to obtain an estimate for the duration of an event given the peak flux or fluence. As the distributions used for durations (the Lévy distribution) and peak flux/fluence (the cut-off power law) are very different, an analytical solution for this regression was not possible. Observing that the higher flux events also tend to have longer duration, a numerical solution can be applied. A random number between 0 and 1 is generated, and this is applied to the distribution function of the cut-off power law (7). By applying this same random number to the distribution function of the Lévy distribution [found by integrating (4)], an event duration can be found. By plotting all the recorded active year events from the event list above, the channel threshold and the residuals compared to the regression fit a measure of the variance of departures was found. The distribution of natural logarithm of the residuals was fit by the normal distribution (which in itself is an indication that the numerical fit is appropriate). During model runs, a random (normal) variable generated using the standard deviation of these residuals is applied to the fitted duration found using the numerical regression.

Fig. 5 shows the regression of the durations against the event peak flux values for Channel 5. The standard deviation found for this channel was 0.8749. No event duration was allowed to exceed the maximum duration seen in the SEPEM Reference Event List. As this value was 44.77 days, generating a residual based on the natural logarithm creates the possibility of very long events ($>$100 days), which could result in an underprediction of peak flux (fluence) as observed events do not last this length of time. In the case that a duration higher than the sample maximum was generated, the random deviation from the numerical regression was regenerated without resampling the event peak flux (fluence).

Table XI shows the correlation coefficients for the regression of event duration with fluence and peak flux. This shows that the characteristics are correlated albeit weakly and that overall there the durations is better correlated to that peak flux than the event fluence. These results give lower values than the 0.56 found by

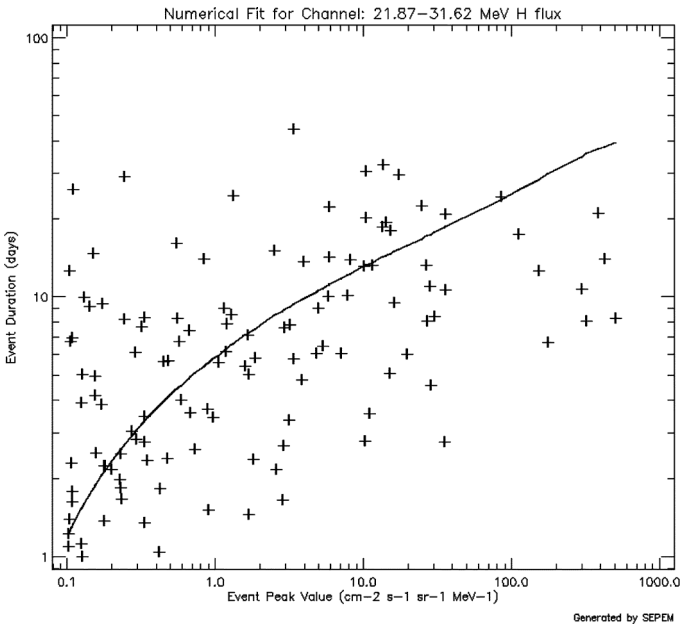

Fig. 5. Regression of durations with Channel-5 peak fluxes.

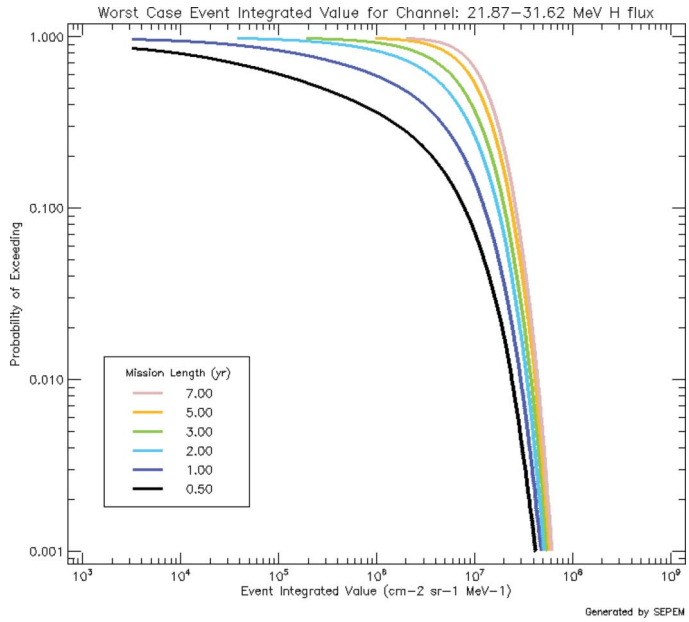

Fig. 6. Worst-case event fluence for Channel 5.

TABLE XI
CORRELATION COEFFICIENT (r^2) FOR REGRESSION OF EVENT DURATION WITH FLUX

	Fluence	Peak Flux
1	0.397	0.438
2	0.402	0.446
3	0.371	0.456
4	0.360	0.404
5	0.326	0.375
6	0.326	0.358
7	0.265	0.312
8	0.281	0.318
9	0.261	0.410
10	0.234	0.322
Mean	0.322	0.384

Jun *et al.* [19]; this could be due to the different event definitions used.

VII. RESULTS

To attain the model results using the SEPEM methodology, a large number of virtual timelines are produced. The Lévy waiting time distribution is randomly sampled to find the time of occurrence of the first event. The cut-off power law is then randomly sampled to find the fluence (peak flux) of the event. The fluence (peak flux) is used to determine the fitted event duration with a random scatter applied. A second waiting time is found by random sampling of the Lévy distribution. The whole process is repeated until the complete mission duration (e.g., 1 year or 7 years) is accounted for by the summation of all the waiting times and event durations in the timeline. The highest peak flux generated, the largest event fluence generated, or the summed fluences from all the events are stored in a vector of length equal to the total number of iterations (timelines) run, which provides the model output. These outputs represent the three types of results that can be generated through the probabilistic method presented in this paper, respectively:

- *Worst-case peak flux:* the flux that will not be exceeded over the mission at a given confidence;
- *Worst-case event fluence:* the integrated flux (fluence) that will not be exceeded by any single SEP event over the mission at a given confidence;
- *Cumulative mission fluence:* the total integrated flux (fluence) that will not be exceeded over the mission at a given confidence.

The values of the parameters for a given confidence level can now be found (by running a large number of iterations—100 000 were used for this work). To do this, the vector for the parameter of interest is sorted in ascending order and plotted against a vector of uniformly distributed values in the range [0, 1] that, in descending order, represents the likelihood of exceeding a stated value (this is one minus the confidence level). The plots for different energies are purposefully represented in this way to match the way the JPL model [6], [7] results were represented and to what users are accustomed. For this work, the mission duration (length of each virtual timeline) was varied to produced results for 1, 2, 3, 5, and 7 years (same as JPL) as well as 0.5 years, which is permissible only due to the new methodology that considers the duration of the SEP events.

As an example, Fig. 6 gives the event fluence on the abscissa for which the probability of it being exceeding within a stated mission duration is given by the ordinate. The largest fluence of a single event will not exceed the given value with confidence of one minus the likelihood given by the ordinate. It is important to consider that this fluence value can be delivered to the spacecraft over a period of 45 days (7.5 weeks), although it is likely due to the nature of the most severe SEP events that the bulk of this will be delivered in a far shorter period of time (a matter of days).

Table XII shows a selection of results for each of the model outputs at three confidence levels (90%, 95%, and 97.5%) for the fifth SEPEM energy channel (21.87–31.62 MeV).

TABLE XII
MODEL RESULTS FOR CHANNEL 5 (21.87–31.62 MeV)

Mission Duration	Confidence 90%	95%	97.5%
Worst-case peak flux ($cm^{-2}s^{-1}sr^{-1}MeV^{-1}$)			
0.5 years	1.97E+2	3.32E+2	4.79E+2
1 years	3.21E+2	4.61E+2	6.08E+2
2 years	4.63E+2	6.11E+2	7.56E+2
3 years	5.44E+2	6.93E+2	8.39E+2
5 years	6.48E+2	8.02E+2	9.58E+2
7 years	7.20E+2	8.74E+2	1.03E+3
Worst-case event fluence ($cm^{-2}sr^{-1}MeV^{-1}$)			
0.5 years	7.99E+6	1.26E+7	1.77E+7
1 years	1.27E+7	1.78E+7	2.30E+7
2 years	1.76E+7	2.25E+7	2.76E+7
3 years	2.04E+7	2.55E+7	3.09E+7
5 years	2.40E+7	2.94E+7	3.47E+7
7 years	2.66E+7	3.19E+7	3.74E+7
Cumulative mission fluence ($cm^{-2}sr^{-1}MeV^{-1}$)			
0.5 years	9.51E+6	1.49E+7	2.07E+7
1 years	1.71E+7	2.37E+7	3.00E+7
2 years	2.82E+7	3.60E+7	4.37E+7
3 years	3.83E+7	4.71E+7	5.55E+7
5 years	5.59E+7	6.62E+7	7.59E+7
7 years	7.26E+7	8.44E+7	9.52E+7

A. Solar Minimum Results

In addition to the results for solar maximum, as mentioned earlier a method for predicting likely fluxes for missions or parts of missions during solar minimum has been established. The key assumption here is that the event size (in terms of flux) is independent of solar cycle period, but that the frequency of significant events varies. Recent large events during solar minimum such as that in December 2006 support this assumption, although this was questioned by Xapsos *et al.* [25] who postulated that during solar minimum not only are the event frequencies smaller, but that "the event magnitudes are smaller, and the energy spectra are softer." However, if event magnitudes are smaller than those at solar maximum, then this model will be conservative, which is a better scenario than risking the opposite possibility in which spacecraft could be underdesigned and fail as a result of effects from SEPs before the mission had run its course. Fig. 7 shows a spectra of cumulative fluence for 0.5, 1, 2, 3, and 4 solar minimum years at a 90% confidence across the modeled energy range.

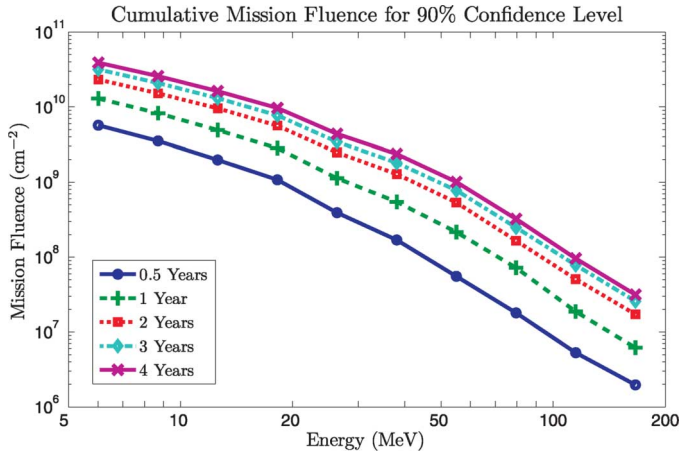

Fig. 7. Integrated mission cumulative fluence spectra for 90% confidence level (solar minimum).

VIII. DISCUSSION

For this work, a new distribution, namely the Lévy distribution, has been applied to the event time distributions. Earlier models (e.g., [7], [10], and [12]) used a Poisson distribution to model event occurrence. Considering the time distribution of CMEs, Wheatland [22] found that a time-dependent Poisson distribution fit the data well. However, analysis by Lepreti *et al.* [26] found that solar flares (a connected process) were better modeled using a Lévy distribution than the time-dependent Poisson distribution that had previously been suggested for this by Wheatland [21]. In previous work [16], it has been shown that SEP events are not random in time, regardless of the definition of an event used, and that the Lévy distribution is also the most robust choice of distribution over various event definitions. This supports the use of the Lévy distribution to model both waiting times and event durations in this work. Analysis of the residuals for this distribution compared to a Poisson and time-varying Poisson distribution presented in Section IV gives strong validation of this choice.

The inclusion of the event durations fitted with an exponential distribution was previously performed by Jun *et al.* [19]. Here, the Lévy distribution was selected based on the goodness-of-fit parameters. The duration was also linked to the fluence and peak flux of the event generated, although the correlation is weak, and therefore the choice to make this connection could be disputed. What should not be disputed is the choice to account for the duration of events. Failure to account for the duration gives rise to the possibility of short time periods with a great many events that may not be feasible as the events in the sample must be extracted from a single time series and therefore may not overlap. This in turn results in an overprediction of fluences at high confidences.

The desire to create more realistic scenarios in the modeling drives the choice of using *virtual timelines* as opposed to the traditional Monte Carlo methods, although a similar number of iterations are required.

It was shown in Section V that two power law distributions give superior fits to the event fluence and peak flux data lognormal distribution. The χ^2 parameter showed little to choose between the truncated power law introduced by Xapsos *et al.* [15] and the power law introduced by Nymmik [24], which we have termed the (exponential) cut-off power law. The choice of the latter of these two distributions was therefore philosophical. For the data generated using the SEPEM reference dataset and the SEPEM event definition, the "design limit" of the truncated power law was found to be very close to the largest event in the list. As it is believed that historically significantly larger events have occurred such as the "Carrington Event" [23], it was decided to use the cut-off power law, which allowed for the possibility of larger events than those observed between 1973 and 2009.

In order to perform some comparisons to other models, it is important to separate the contribution to any differences made by the data from that of the modeling methodology. Fig. 8 shows a comparison of the JPL, ESP, and SEPEM modeling methods

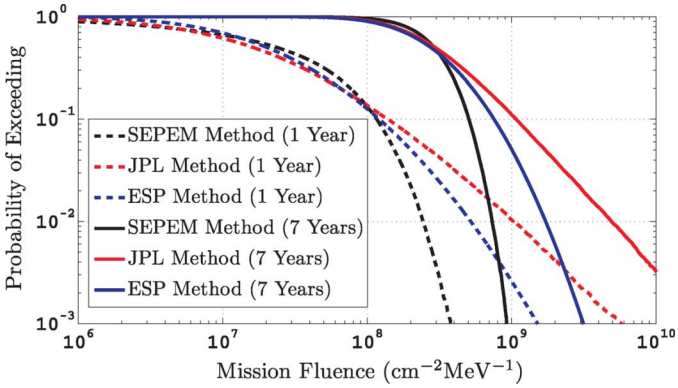

Fig. 8. 1-year and 7-year comparisons of modeling methods using SEPEM dataset.

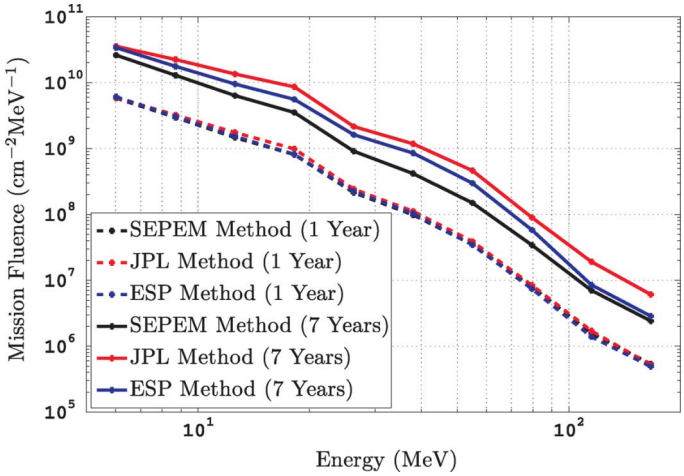

Fig. 9. Comparison of methods for mission cumulative fluence spectra with 90% confidence level using the SEPEM dataset.

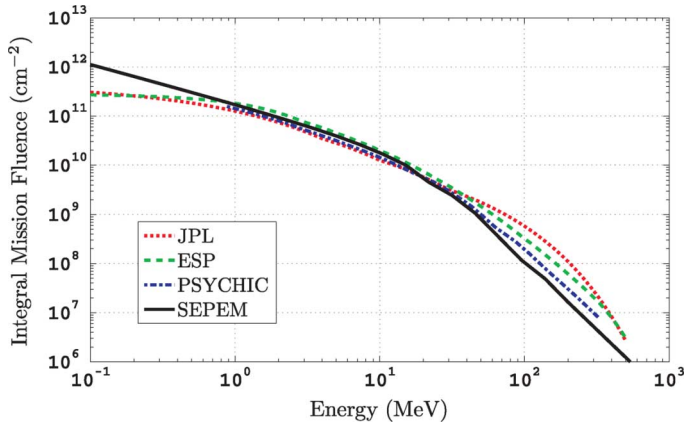

Fig. 10. Comparison of models for 1-year mission cumulative fluence spectra with 90% confidence level.

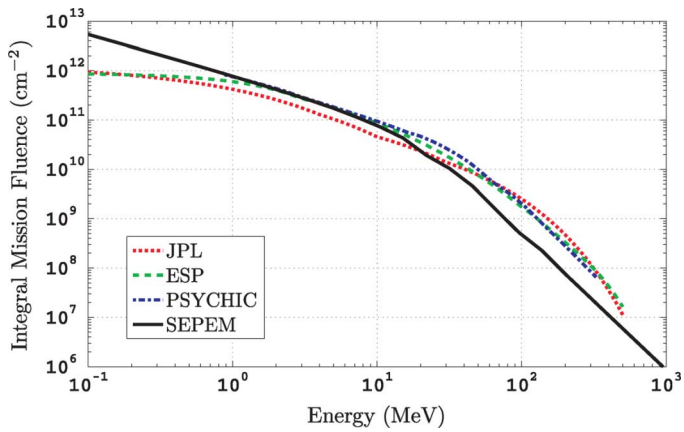

Fig. 11. Comparison of models for 7-year mission cumulative fluence spectra with 90% confidence level.

for calculating cumulative mission fluences using data from the third SEPEM channel for 1-year and 7-year missions.

The differences of the methods are clear to see with the JPL method giving the harshest environment predictions at high confidence (low probability of exceeding), then the ESP method, and finally the SEPEM method. However, for the widely used 90% confidence, the 1-year predictions are all very similar. Unfortunately, there are noticeable differences for the 7-year outputs at this confidence level. The differences between SEPEM and JPL can be traced to the fluence distributions used. For longer missions, the chances that a very rare event is generated increase, and the size of these events is markedly different for the lognormal and cut-off power-law distributions. The differences between SEPEM and the ESP method are harder to determine as the methods are quite different, but the ESP assumption of Poisson-distributed events to extend outputs to mission durations other than 1 year may lead to harsher >1-year fluences. The Lévy distribution considers that the highest yearly fluences are due to a strong clustering of events. Over longer mission durations, this clustering will even out, resulting in lower fluences than for an extrapolation following the assumption that the events are random in time. Another factor may be the deviation from a pure power law [14], [24] for the largest events that can dominate; it is not clear how this was incorporated into the ESP cumulative fluence method [12]. Fig. 9 shows the spectra for the JPL, ESP, and SEPEM modeling methods applied to the SEPEM dataset for 90% confidence. As seen in Fig. 8, there is very little difference for the 1-year models using the same dataset. However, there are significant differences for the 7-year predictions as explained above.

A comparison of 90% confidence model results as implemented on SPENVIS[3] for the JPL model (JPL-91) and the ESP model, generated using data provided by Xapsos for PSYCHIC, and the SEPEM dataset for the SEPEM model is shown in Figs. 10 and 11 for 1- and 7-year mission, respectively. The SEPEM model has been extended in energy using two power-law approximations: 1 for below 5 MeV and one for above 200 MeV. This is based on the observations of spectra of individual SEP events by Mewaldt *et al.* [11], which was based on previous work in relation to gamma ray bursts by Band *et al.* [27]. However, the model shows a smoother transition over the range from 10 to 100 MeV as there are a combination of events with transitions from one power law to the next at different energies in each model run. The differential results have then been integrated with energy as this is the form that most published models take.

[3]http://www.spenvis.oma.be/

TABLE XIII
COMPARISON OF MODEL RESULTS FOR TOTAL MISSION INTEGRAL FLUENCES

	>10 MeV	>25 MeV	>50MeV	>100 MeV
1 year - 90% confidence				
JPL	1.250E+10	4.240E+09	1.770E+09	5.790E+08
ESP	1.970E+10	5.160E+09	1.460E+09	3.220E+08
PSYCHIC	1.430E+10	4.141E+09	1.000E+09	1.945E+08
SEPEM	1.775E+10	3.620E+09	8.095E+08	1.053E+08
1 year - 95% confidence				
JPL	2.120E+10	7.600E+09	3.320E+09	1.150E+09
ESP	3.510E+10	1.020E+10	3.080E+09	7.090E+08
PSYCHIC	2.427E+10	8.332E+09	2.262E+09	4.629E+08
SEPEM	2.418E+10	5.163E+09	1.190E+09	1.640E+08
7 years - 90% confidence				
JPL	4.540E+10	1.780E+10	7.680E+09	2.500E+09
ESP	8.570E+10	2.520E+10	7.600E+09	1.730E+09
PSYCHIC	9.407E+10	3.513E+10	9.856E+09	2.009E+09
SEPEM	7.673E+10	1.544E+10	3.511E+09	4.742E+08
7 years - 95% confidence				
JPL	6.610E+10	2.810E+10	1.250E+10	4.110E+09
ESP	1.300E+11	4.280E+10	1.390E+10	3.360E+09
PSYCHIC	1.340E+11	5.879E+10	1.886E+10	4.070E+09
SEPEM	8.863E+10	1.818E+10	4.183E+09	5.738E+08

Fig. 10 shows good agreement between the model outputs from >1 up to >30 MeV, but greater variation above this energy threshold possibly, in part, due to fewer significant events at these energies, resulting in greater scatter for the distributions used. The values below >1 MeV are extrapolated, and the implementation of the extrapolation in SPENVIS[4] has not been published in the JPL or ESP papers. These data are included for completeness and because users may be interested in the SEPEM model predictions in this energy range for missions outside the magnetosphere, but are not model results in the case of JPL or ESP. The PSYCHIC model is based only on data with no extrapolation, and this shows the closest agreement with the SEPEM model most likely because of the care taken in processing the data and the inclusion of more recent data from solar cycle 23 in both cases.

Fig. 11 shows poorer agreement in general for reasons outlined above, but in the 1–10 MeV range, the agreement is better at least between the ESP, PSYCHIC, and SEPEM models.

Table XIII shows the results for 4 integral energy channels (>10, >25, >50, >100 MeV); this required an interpolation in some cases. Some values could be recommended for "standard" near-Earth missions by an averaging of model outputs, which would be of great help to the users of these long-term climatological SEP environment models. However, ultimately further comparison is required to determine the sources of the differences between models and to resolve those differences.

IX. CONCLUSION

A new model of solar energetic particle peak fluxes and fluences has been created as a part of the ESA SEPEM Project. This model is based on the carefully processed dataset that is both homogenous and covering of a long time span. The method using virtual timelines has allowed the incorporation of event durations in a way similar to that of Jun *et al.* [19].

[4]Since the analyses for this paper were performed, the extrapolation for the ESP model has been changed from a exponential with energy to a power law with energy such as performed for the SEPEM model extrapolation.

The fluence and peak flux distribution function is based upon that of Nymmik [24], which includes a deviation from a power law as noted by Xapsos *et al.* [15] following earlier work on power-law fits to SEP event fluences by Gabriel and Feynman [28]. The waiting times and event durations are fitted using a Lévy distribution applied to solar-flare waiting times by Lepreti *et al.* [26] as described in previous work [16]. For solar minimum calculations, the waiting time distributions used are time-dependent Poisson distributions as described by Wheatland [22]. This model can be seen as an evolution of previous work covering over three decades beginning with analysis performed by King and published in 1974 [5]. The major challenge associated with SEP modeling remains to provide reliable environment predictions despite limitations of the data in both its time span and reliability. However, in this work, the available data, method, and distributions required to provide long-term climatological predictions of the likely mission cumulated fluence, worst-case event fluence, and worst-case peak flux have been studied in great detail in order to provide a reliable model for use by spacecraft designers and operators.

Work is being carried out to better integrate the SEPEM model with the effects tools used by spacecraft designers, which may provide more reliable dose and SEE rate predictions and also to better estimate interplanetary fluxes away from 1 AU. Data browsing and processing, statistical models, effects tools, and supporting information are accessible on the SEPEM application server Web page: http://dev.sepem.oma.be/. This includes the functionality to produce results using other data and well-known models or to combine distributions and methodologies from different models forming the user's own composite model. More reliable models of the SEP environment enable greater security of space assets and/or savings in weight and therefore cost of launches.

ACKNOWLEDGMENT

The authors would like to acknowledge the work done by other partners in the SEPEM consortium at Universitat de Barcelona, Katholieke Universiteit Leuven, and QineitQ on the other aspects of the SEPEM project, and Dr. M. Xapsos for providing his complete dataset and explanations regarding its creation.

REFERENCES

[1] D. V. Reames, "Particle acceleration at the sun and in the heliosphere," *Space Sci. Rev.*, vol. 90, pp. 413–491, 1999.
[2] A. J. Tylka, W. F. Dietrich, and P. R. Boberg, "Probability distributions of high-energy solar-heavy-ion fluxes from IMP-8: 1973–1996," *IEEE Trans. Nucl. Sci.*, vol. 44, no. 6, pp. 2 140–2 149, Dec. 1997.
[3] M. A. Xapsos, C. Stauffer, T. Jordan, J. L. Barth, and R. A. Mewaldt, "Model for cumulative solar heavy ion energy and linear energy transfer spectra," *IEEE Trans. Nucl. Sci.*, vol. 54, no. 6, pp. 1 985–1 989, Dec. 2007.
[4] J. Feynman and S. B. Gabriel, "On space weather consequences and predictions," *J. Geophys. Res.*, vol. 105, no. A5, pp. 10 543–10 564, 2000.
[5] J. H. King, "Solar proton fluences for 1977–1983 space missions," *J. Spacecraft Rockets*, vol. 11, no. 6, pp. 401–408, 1974.
[6] J. Feynman, T. P. Armstrong, L. Dao-Gibner, and S. Silverman, "A new interplanetary fluence model," *J. Spacecraft Rockets*, vol. 27, no. 4, pp. 403–410, 1990.

[7] J. Feynman, G. Spitale, J. Wang, and S. B. Gabriel, "Interplanetary proton fluence model: JPL 1991," *J. Geophys. Res.*, vol. 98, no. A8, pp. 13 281–13 294, 1993.
[8] J. Feynman, A. Ruzmaikin, and V. Berdichevsky, "The JPL proton fluence model: An update," *J. Atmosph. Solar-Terr. Phys.*, vol. 64, no. 16, pp. 1 679–1 686, 2002.
[9] L. Rosenqvist, A. Hilgers, H. Evans, E. Daly, M. Hapgood, R. Stamper, R. Zwickl, S. Bourdarie, and D. Boscher, "Toolkit for updating interplanetary proton-cumulated fluence models," *J. Spacecraft Rockets*, vol. 42, no. 6, pp. 1 077–1 090, 2005.
[10] R. A. Nymmik, "Probabilistic model for fluences and peak fluxes of solar energetic particles," *Radiat. Meas.*, vol. 30, no. 3, pp. 287–296, 1999.
[11] R. A. Mewaldt, C. M. S. Cohen, A. W. Labrador, R. A. Leske, G. M. Mason, M. I. Desai, M. D. Looper, J. E. Mazur, R. S. Selesnick, and D. K. Haggerty, "Proton, helium and electron spectra during the large solar particle events of October–November 2003," *J. Geophys. Res.*, vol. 110, p. A09S18, 2005.
[12] M. A. Xapsos, G. P. Summers, J. L. Barth, E. G. Stassinopoulos, and E. A. Burke, "Probability model for cumulative solar proton event fluences," *IEEE Trans. Nucl. Sci.*, vol. 47, no. 3, pp. 486–490, Jun. 2000.
[13] M. A. Xapsos, G. P. Summers, and E. A. Burke, "Extreme value analysis of solar energetic proton peak fluxes," *Solar Phys.*, vol. 183, pp. 157–164, 1998.
[14] M. A. Xapsos, G. P. Summers, J. L. Barth, E. G. Stassinopoulos, and E. A. Burke, "Probability model for worst case solar proton event fluences," *IEEE Trans. Nucl. Sci.*, vol. 46, no. 6, pp. 1 481–1 485, Dec. 1999.
[15] M. A. Xapsos, G. P. Summers, and E. A. Burke, "Probability model for peak fluxes of solar proton events," *IEEE Trans. Nucl. Sci.*, vol. 45, no. 6, pp. 2 948–2 953, Dec. 1998.
[16] P. T. A. Jiggens and S. B. Gabriel, "Time distributions of solar energetic particle events: Are SEPEs really random?," *J. Geophys. Res.*, vol. 114, no. A10, p. A10105, 2009.
[17] I. N. Myagkova, M. I. Panasyuk, L. L. Lazutin, E. A. Muravieva, L. I. Starostin, T. A. Ivanova, N. N. Pavlov, I. A. Rubinshtein, N. N. Vedenkin, and N. A. Vlasova, "December 2006 solar extreme events and their influence on the near-earth space environment: Universitetskiy-tatiana satellite observations," *Adv. Space Res.*, no. 4, pp. 489–494, 2009.
[18] J. Feynman, A. J. Tylka, D. B. Reames, and S. B. Gabriel, "Near-sun energetic particle environment of solar probe—Phase1 final report Jet Propulsion Laboratory, Los Angeles, CA, Tech. Rep., 2000.
[19] I. Jun, R. T. Swimm, A. Ruzmaikin, J. Feynman, A. J. Tylka, and W. F. Dietrich, "Statistics of solar energetic particle events: Fluences, durations and time intervals," *Adv. Space Res.*, vol. 40, pp. 304–312, 2007.
[20] M.-H. Y. Kim, M. J. Hayat, A. H. Feiveson, and F. A. Cucinotta, *Health Phys.*, vol. 97, no. 1, pp. 68–81, 2009.
[21] M. S. Wheatland, "The origin of the solar flare waiting-time distribution," *Astrophys. J.*, vol. 536, pp. L109–L112, 2000.
[22] M. Wheatland, "The coronal mass ejection waiting-time distribution," *Solar Physics*, vol. 214, pp. 361–373, 2003.
[23] R. C. Carrington, "Description of a singular appearance seen on the sun on September 1, 1859," *Monthly Notices Roy. Astronom. Soc.*, vol. 20, pp. 13–15, 1860.
[24] R. A. Nymmik, "Some problems with developing a standard for determining solar energetic particle fluxes," *Radiat. Meas.*, vol. 47, pp. 622–628, 2011.
[25] M. A. Xapsos, C. Stauffer, G. B. Gee, J. L. Barth, E. G. Stassinopoulos, and R. E. GcGuire, "Model for solar proton risk assessment," *IEEE Trans. Nucl. Sci.*, vol. 51, no. 6, pp. 3 394–3 398, Dec. 2004.
[26] F. Lepreti, V. Carbone, and P. Veltri, "Solar flare waiting time distribution: Varying rate-Poisson or Lévy function?," *Astrophys. J.*, vol. 555, pp. L113–L136, 2001.
[27] D. Band, J. Matteson, L. Ford, B. Schaefer, D. Palmer, B. Teegarden, T. Cline, M. Briggs, W. Paciesas, G. Pendleton, G. Fishman, C. Kouveliotou, C. Meegan, R. Wilson, and P. Lestrade, "BATSE observations of gamma-ray burst spectra. I—Spectral diversity," *Astrophys. J.*, vol. 413, no. 1, pp. 281–292, 1993.
[28] S. B. Gabriel and J. Feynman, "Power-law distribution for solar energetic proton events," *Solar Phys.*, vol. 165, no. 2, pp. 337–346, 1996.